New ideas in $b \to s\ell\ell$ transitions

Unbinned, $B \to K^{(*)}\tau\tau$, Inclusive vs. Exclusive Observables and the C_9 Dilemma

Joaquim Matias

June 20, 2026

Flavorful opportunities in Semileptonic B decays.

Outline of the Talk

- Unbinned model-independent analysis of $B \to K^*(\to K\pi)\ell\ell$
- Hadronic Resonance impact on $B \to K^{(*)}\tau\tau$
- Probing unknown nonperturbative effects in $b \to s\ell\ell$ with inclusive and exclusive modes

A model-independent unbinned analysis of $B \to K^*(\to K\pi)\mu\mu$

Accessing $b \to s\ell\ell$ data in a different way

Bernat Capdevila, Joaquim Matias, Martin Novoa-Brunet, Mitesh Patel and Mark Smith

based on Phys. Rev. D112 (2025) 1, 016007

Flavorful opportunities in Semileptonic B decays.

$B \to K^*\mu^+\mu^-$: Optimized Binned Observables

- Until recently all the information on the 4-body angular distribution $B \to K^*(\to K\pi)\mu^+\mu^-$ was provided in bins of lepton pair invariant mass (q^2).
- The analysis of this information provided by LHCb, Belle, ATLAS and finally also CMS, led us to the identification of the most prominent and persistent anomaly: the observable P_5'.

Previous to 2024

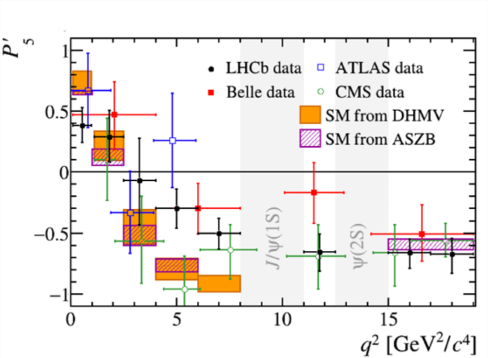

2024

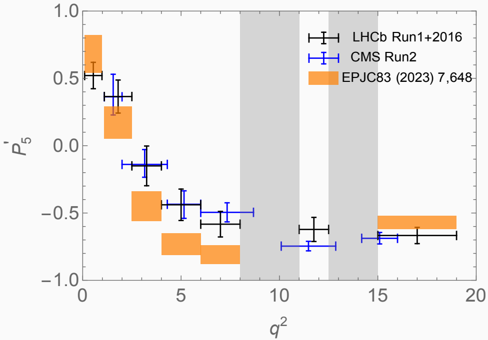

Unbinned optimized observables

The unbinned definitions of the observables: **[Capdevila et al. 2504.00949]**

$$\mathbf{P}_2(\mathbf{q}^2) = \frac{1}{8}\frac{[J_{6s}+\bar{J}_{6s}]}{[J_{2s}+\bar{J}_{2s}]}\ , \quad \mathbf{P}_4'(\mathbf{q}^2) = \frac{1}{\mathcal{N}'}[J_4+\bar{J}_4]\ , \quad \mathbf{P}_5'(\mathbf{q}^2) = \frac{1}{2\mathcal{N}'}[J_5+\bar{J}_5]$$

$$\text{with } \mathcal{N}' = \sqrt{-(J_{2s}+\bar{J}_{2s})(J_{2c}+\bar{J}_{2c})}$$

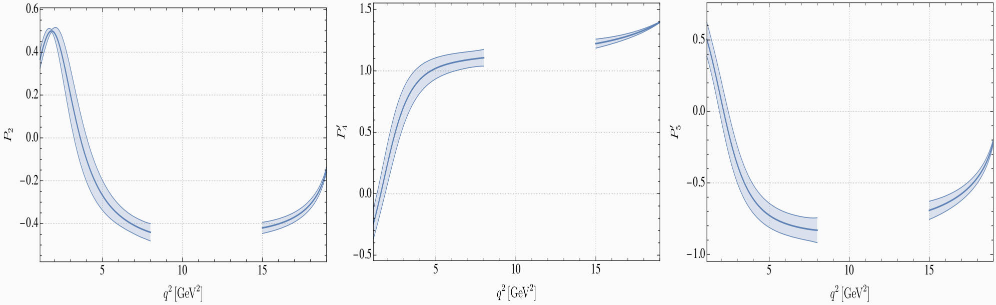

We have checked that binning the MC samplings used recover our binned observables predictions.

Unbinned observables: Amplitude parametrizations

$\Rightarrow$ Amplitude parametrizations:

[R. Aaij et al. 2312.09115, N. Gubernari at al., 2011.09813, 2206.03797, R. Aaij at al. 2405.17347, N. Gubernari et al. 2305.06301]

- Model for local and non-local contributions:

$$\mathcal{A}_\lambda^{L,R} = \mathcal{N}_\lambda \left\{ \left[(C_9 \pm C_9') \mp (C_{10} \pm C_{10}') \right] \mathcal{F}_\lambda(q^2) + \frac{2m_b m_B}{q^2} \left[(C_7 \pm C_7')\mathcal{F}_\lambda^T(q^2) - 16\pi^2 \frac{mB}{m_b} \mathcal{H}_\lambda(q^2) \right] \right\}$$

$\lambda = \perp, \|, 0$. $\mathcal{F}_\lambda^{(T)}$ Form factors and $\mathcal{H}_\lambda$ non-local correlator ¸charm-loop".

z-expansion + ($\mathcal{B}(B \to K^* J/\psi)$ and $\mathcal{B}(B \to K^* \psi(2S))$ constraints.

Two hypotheses are considered for the data included in the fit:

(i) $q^2 < 0$, where theory constraints coming from the light-cone OPE are included;

(ii) $q^2 > 0$, where these constraints are excluded.

$\Rightarrow$ A model-independent moments method: Observable parametrization.

Which conditions define a good amplitude parameterization?

Conditions to test a theoretical parametrization: Counting d.o.f.

[B. Capdevila et al. 2504.00949,M- Alguero et al. 2107.05301]

$$2n_A - n_{sym} = n_c - n_{rel} = n_{dof}$$

- **Massless case:** 8 d.o.f. ($n_c = 11$ coefficients, $n_{sym} = 4$, $\mathrm{n}_A = 6$: $A^{L,R}_{\perp,\parallel,0}$)
  - There are 3 relations (2 trivial and one non-trivial between observables)
  - There are 8 conditions.
- **Massive case:** 10 d.o.f. ($n_c = 11$ coefficients, $n_{sym} = 4$, $n_A = 7$: $A^{L,R}_{\perp,\parallel,0}$, A_t)
  - There is only 1 relation (non-trivial between observables)
  - There are 10 conditions.
- **Massive case+scalar:** 12 d.o.f. ($n_c = 12$ coefficients, $n_{sym} = 4$, $n_A = 8$: $A^{L,R}_{\perp,\parallel,0}$, A_t, A_S)
  - There is no relation (non-trivial relation between observables is broken)

Conditions to test a theoretical parametrization: I

To define these conditions (for the P-wave) is instrumental to use a set of three complex 2-component vectors defined:

$$n_{\|} = \begin{pmatrix} A_{\|}^{L} \\ A_{\|}^{R*} \end{pmatrix}, \quad n_{\perp} = \begin{pmatrix} A_{\perp}^{L} \\ -A_{\perp}^{R*} \end{pmatrix}$$

$$n_0 = \begin{pmatrix} A_0^{L} \\ A_0^{R*} \end{pmatrix},$$

Two more for S-wave.

	THEORY		EXPERIMENT
$\mathrm{Cond.}_1:$	$\lvert n_{\perp}\rvert^2$	$=$	$\frac{2}{\beta^2}J_{2s} + \frac{1}{\beta^2}J_3$
$\mathrm{Cond.}_2:$	$\lvert n_{\|}\rvert^2$	$=$	$\frac{2}{\beta^2}J_{2s} - \frac{1}{\beta^2}J_3$
$\mathrm{Cond.}_3(\mathrm{Re\,and\,Im}):$	$n_{\|}^{\dagger} n_{\perp}$	$=$	$\frac{1}{2\beta}J_{6s} + i\frac{1}{\beta^2}J_9$
$\mathrm{Cond.}_4(\mathrm{Re\,and\,Im}):$	$n_{\|}^{\dagger} n_0$	$=$	$\frac{\sqrt{2}}{\beta^2}J_4 + \mathbf{i}\frac{\mathbf{1}}{\beta\sqrt{\mathbf{2}}}\mathbf{J_7}$
$\mathrm{Cond.}_5(\mathrm{Re\,and\,Im}):$	$n_{\perp}^{\dagger} n_0$	$=$	$\frac{1}{\beta\sqrt{2}}J_5 + i\frac{\sqrt{2}}{\beta^2}J_8$

and two massive ones (Condition 6 and 7)

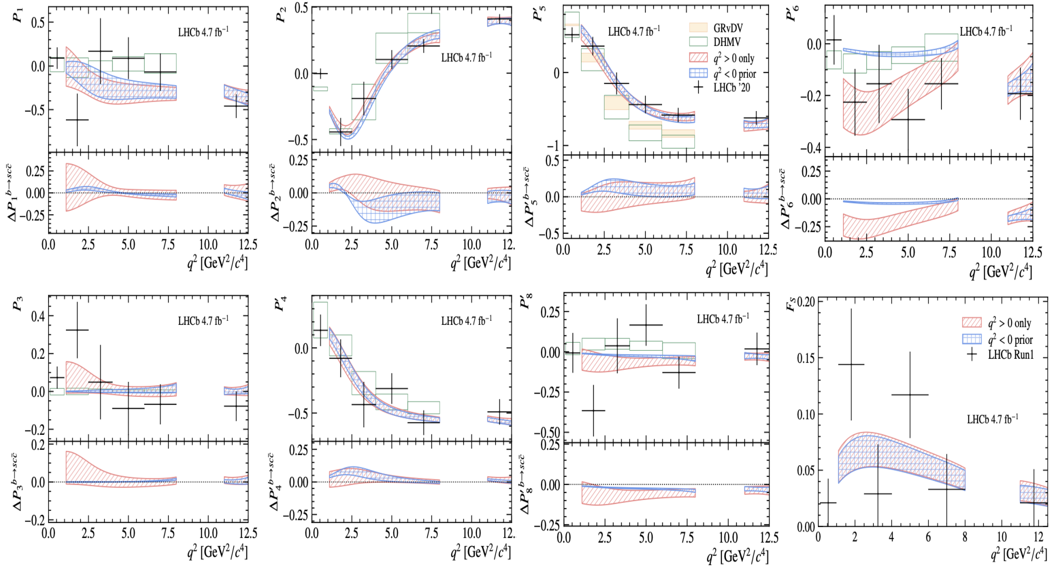

[A. Mauri, Santiago de Compostela, CKM 2023]

Conditions to test a theoretical parametrization: II

Notice reverse colors w.r.t Andrea Mauri plots!!!

Fit to data using only $q^2 > 0$ points + lattice ("Fit I"). This fit **in blue here** (red in Andreas' plots) reproduces very well the binned data (real and imaginary). All conditions OK. No problem in P_6'.

Fit to data including $q^2 < 0$ points + lattice ("**Fit II**"). This fit **in red here** (blue in Andreas' plots) is highly impacted by theory points at $q^2 < 0$ and **it is tension with data** (problem in imaginary condition 4). Problem in P_6' ($\mathrm{Im}(A_{\parallel})$).

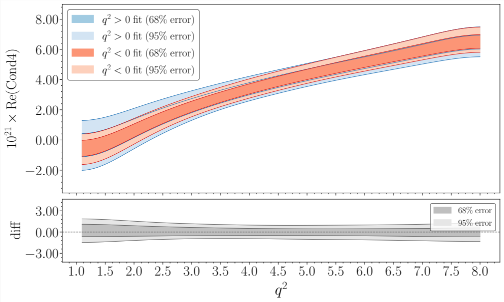

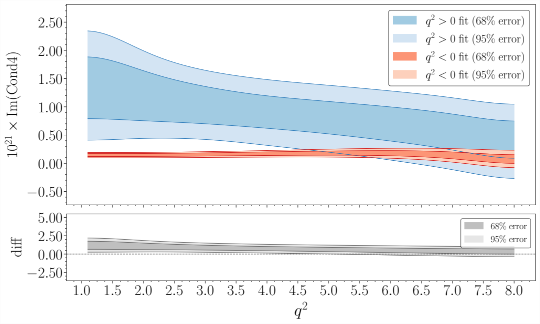

[B. Capdevila et al. 2504.00949, W. Altmannshofer et al. 2603.27753]

This discrepancy indicates a possible problem in the parameterisation of $\mathrm{Im}(n_\parallel^\dagger n_0)$.

Several reasons can be behind this problem (if real):

- The strong phases fixed using theory at $q^2 < 0$ are in tension with the $B \to K^*(\to K^+\pi^-)\mu^+\mu^-$ data, maybe because higher-order corrections to them are needed;
- There is a problem in a) the extrapolation to positive q^2 or b) the lattice calculation.
- There is an exp problem in the extraction of this particular observable or a fluctuation.

Notice that $\mathrm{Im}A_i^L = \mathrm{Im}A_i^R$ (with $i = \perp, \parallel, 0$).

which implies that

$$\begin{aligned} J_5 &= \sqrt{2}\beta(\mathrm{Re}A_0^L\mathrm{Re}A_\perp^L - \mathrm{Re}A_0^R\mathrm{Re}A_\perp^R), \\ J_{6s} &= 2\beta(\mathrm{Re}A_\parallel^L\mathrm{Re}A_\perp^L - \mathrm{Re}A_\parallel^R\mathrm{Re}A_\perp^R). \end{aligned}$$

Notice: numerator of P_5' and P_2 **their zeroes are unaffected by** $Im[A_i]$ while

$$J_7 = \sqrt{2}\beta(\mathrm{Im}A_\parallel^L(\mathrm{Re}A_0^R - \mathrm{Re}A_0^L) + \mathrm{Im}A_0^L(\mathrm{Re}A_\parallel^L - \mathrm{Re}A_\parallel^R))$$

A new model-independent unbinned method based on the method of moments

Experiment

The method of moments

Up to now experimental angular observables have been: i) binned in q^2 and ii) integrated the observables over the analysis window of $K\pi$.

Most analysis:

- LHCb - $\rightarrow$, 3: http://cds.cern.ch/record/2115087JHEP 02 (2016) 104
- LHCb - $\rightarrow \Lambda$: https://cds.cern.ch/record/2633197JHEP 09 (2018) 146
- LHCb - $\rightarrow$ at high : https://cds.cern.ch/record/2216088JHEP 12 (2016) 065

have all been binned in q^2

"Why don't you just use the moments ?" - Danny / Kostas

Using moments to extract angular observables is not new (in bins): Beaujean, Chrzaszcz, van Dyk, Serra: https://journals.aps.org/prd/abstract/10.1103/PhysRevD.91.114012PRD 91 (2015) 114012

In previous analysis:

Perform a fit of the 3D dimensional angular PDF with:

- observables as fit parameters
- or compute angular moments in each specific fixed bin

Outcome: Complete basis of angular observables

Caveat: binning in q^2 some information on the underlying physics is lost.

Previous attempts to exploit full q^2 dependence: extract theory parameters (WC, FFs..)

.... **this is model-dependent**

Goal: Novel method to extract the set of **model-independent** angular observables want to get more physics out of it.

“Unbinned” moments

Calculate the moments continuously in q^2 with a *knn* regressor:

- The *knn* calculates the rate-normalised, moments of the data for a sampled q^2 point
  - Take the nearest k events to the sampled point
  - Sum their angular functions, divide by k

$$M_i(q^2) = \frac{1}{k}\sum_k f_i(\Omega_j)$$

  - “Unbinned” numerical function of q^2 - really a “continuous” binning
- Now we have a numeric estimation of the moments at any point in q^2 - a continuous numeric function
- We can apply some filtering algorithm to smooth the distribution - i.e. Gaussian Process Regression or Savitzky-Golay filter

For some analyses, such as finding the zero-crossing points in q^2 one may choose a larger number of neighbours, as the zeros lie in a q^2 region where the observables of interest are expected to vary smoothly.

P-wave observables

Pseudo-experiment with 130,000 P-wave events - estimate of LHCb 50(upgrade I)

- Here neglect bkg and acceptance - would treat as per https://journals.aps.org/prd/abstract/10.1103/PhysRevD.91.114012PRD 91 (2015) 114012
- We use the second order moments to calculate the variances and covariances
- Combine extracted S_i, S_2^s and S_2^c for the optimised $P_i^{(\prime)}$ observables

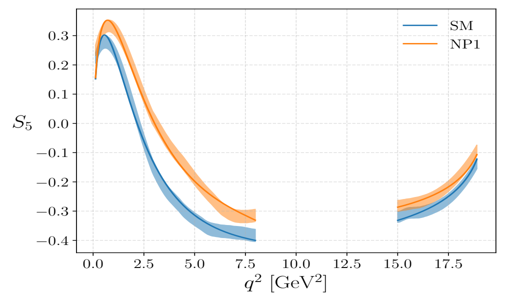

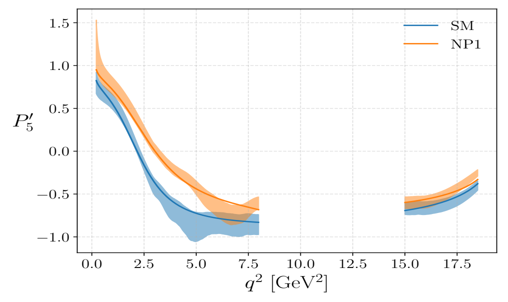

Examples of use of unbinned approach: Bounds, **zeroes** and a relation (... more soon)

Illustrative examples of testing data (theory)

From the definitions of:

$$P_4 = \frac{\mathrm{Re}(n_0^\dagger n_\parallel + \mathrm{CP})}{\sqrt{(|n_\parallel|^2 + \mathrm{CP})(|n_0|^2 + \mathrm{CP})}}, \quad P_6 = \frac{\mathrm{Im}(n_0^\dagger n_\parallel + \mathrm{CP})}{\sqrt{(|n_\parallel|^2 + \mathrm{CP})(|n_0|^2 + \mathrm{CP})}},$$

$$\Rightarrow |P_4 + iP_6|^2 \leq 1 \quad \text{or} \quad |P_4' + i\beta P_6'|^2 \leq 1 - P_1.$$

- New geometrical bounds:

$$|P_2| \leq \frac{1}{2\beta}\sqrt{1 - 4P_3^2}, \quad |P_4'| \leq \sqrt{1 - P_1 - \beta^2 P_6'^2}, \quad |P_5'| \leq \frac{1}{\beta}\sqrt{1 + P_1 - P_8'^2}$$

$$|P_3| \leq \frac{1}{2}\sqrt{1 - 4\beta^2 P_2^2}, \quad |P_6'| \leq \frac{1}{\beta}\sqrt{1 - P_1 - P_4'^2}, \quad |P_8'| \leq \sqrt{1 + P_1 - \beta^2 P_5'^2}$$

$$\Rightarrow \begin{cases} \text{Amplitude parametrization: } \bullet \text{ Fulfilled in SM and NP. Self-consistency test.} \\ \text{Observable parametrization: } \bullet \text{ Test on validity of an experimental unbinned analysis} \end{cases}$$

Illustrative examples of testing data

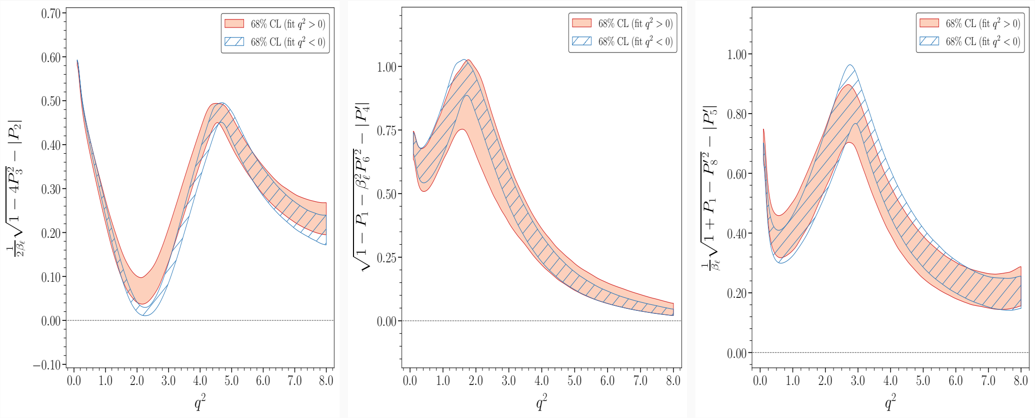

Bounds on optimised observables using the amplitude parametrization in the two cases $q^2 > 0$ (experiment-red) and $q^2 < 0$ (theory-blue).

... P_2 **saturates bound around 2 GeV^2 and** P_4' **around 8 GeV^2.**

Zero-crossing point of P_i observables

- Assuming NP only in C_9 in agreement with the dominant scenario.

[M. Algueró et al., 2304.07330]

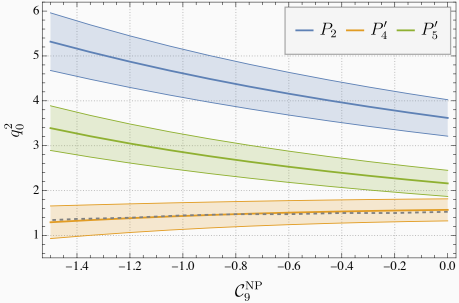

Figura 1: Plot of exact position of the zero of P_2 and $P'_{4,5}$ versus $C_9^{\rm NP}$. The dashed line corresponds to the approximate expression.

- NLO SM prediction zero-crossing points:

$$\begin{aligned} q^2_{0\,|\,P_2} &= 3.60 \pm 0.40 \\ q^2_{0\,|\,P'_4} &= 1.57 \pm 0.25, \\ q^2_{0\,|\,P'_5} &= 2.16 \pm 0.29, \end{aligned}$$

$$[P'_4(q_0^2)^2 + P'_5(q_0^2)^2] = 1 - \eta(q_0^2) \text{ with}$$

$$\eta(q_0^2) = [P_1^2 + P_1({P'_4}^2 - {P'_5}^2)] \text{ for } P_2(q_0) = 0$$

- Zero of P_1 and P'_5 coincide to good accuracy in the SM and diverge with $C_9^{\rm NP} \neq 0$.

Nice from the unbinned exp P'_5 and P_2 one gets $q_0^2 \neq q_0^{2SM}$, i.e., P_2 is $C_9^{\rm NP} \simeq -1.1^{+0.4}_{-0.2}$

Observable zero

Continuous observables are well-suited to finding the zeroes of the observables (use S_i rather than P_i)

P_2 :

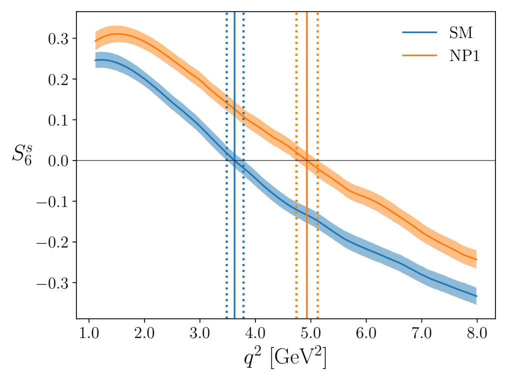

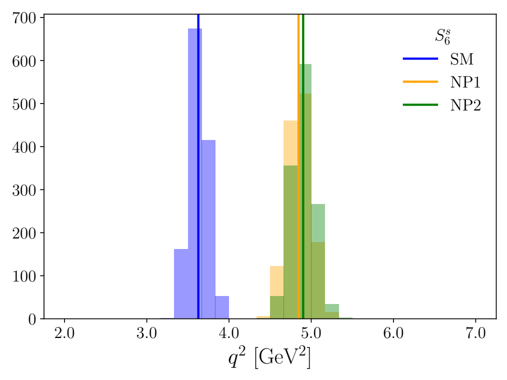

Observable zero

Continuous observables are well-suited to finding the zeroes of the observables (use S_i rather than P_i)

P_5' :

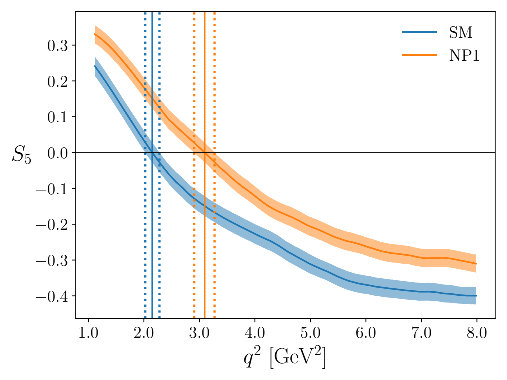

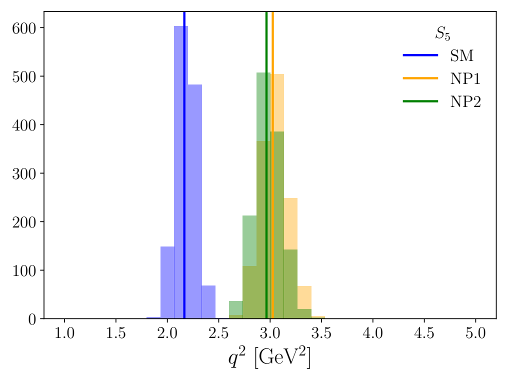

- The known non-trivial relation $J_{2c} = f(J_i)$ in terms of observables:

[U. Egede et al. 1005.0571, N. Serra and J.M, 1402.6855]

$$P_2 = -P_2^{CP} + \frac{1}{2\bar{k}_1}\left[(\bar{P}_4'\bar{P}_5' + \delta_1) + \frac{1}{\beta}\sqrt{\eta + \delta_2 + \delta_3\bar{P}_1 + \delta_4\bar{P}_1^2}\right] \text{ with } \delta_i \simeq 0$$

$$\text{with } \eta = (-1 + P_1 + P_4'^2)(-1 - P_1 + \beta^2 P_5'^2)$$

The simplified version $(P_i^{\rm CP}, P_{3,6,8}^{(\prime)} \to 0) \Rightarrow P_2 = \frac{1}{2}[P_4'P_5' + \frac{1}{\beta}\sqrt{\eta}]$ is very precise.

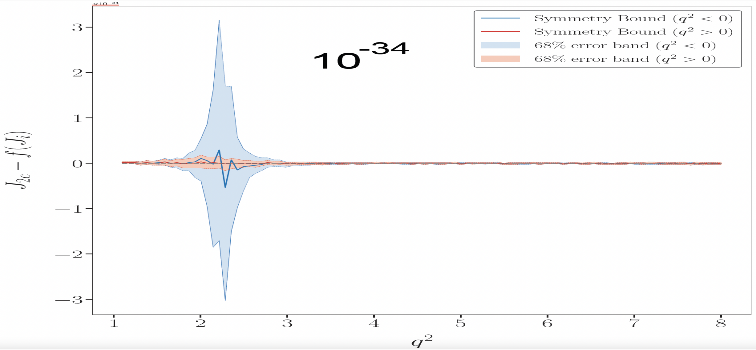

Examples of testing data in presence of scalar

The previous bounds become:

$$|P_5' + \omega_r| \leq \frac{1}{\beta}\sqrt{1 + P_1 - P_8'^2}$$

and

$$|P_6' + \omega_i| \leq \frac{1}{\beta}\sqrt{1 - P_1 - P_4'^2}$$

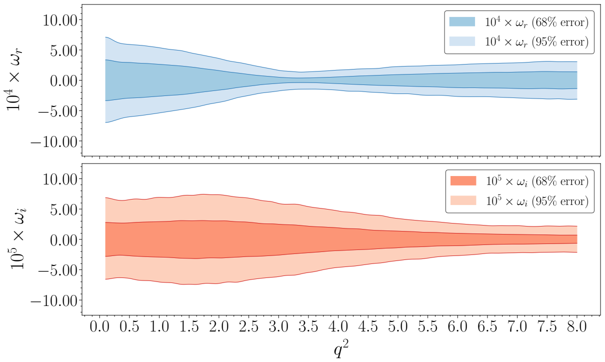

with $\omega_{r,i} = +\frac{1}{N}\sqrt{2}\frac{m_\ell}{\beta\sqrt{q^2}}[\mathrm{Re}/\mathrm{Im}(A_\parallel^L A_S^* + A_\parallel^{R*} A_S) + \mathrm{CP}] \sim \mathcal{O}(10^{-4})$

$$\Rightarrow P_2 = \frac{1}{2}\left[P_4' P_5' + \frac{1}{\beta}\sqrt{\eta}\right] + \Delta \quad \text{with} \quad \Delta = \frac{\omega_r}{2}\left(P_4' - \beta P_5' \sqrt{\frac{-1 + P_1 + P_4'^2}{-1 - P_1 + \beta^2 P_5'^2}}\right)$$

The bounds and relation remain robust even in presence of a scalar due to $\mathcal{B}(B_s \to \mu\mu)$.

$B \to D^*\ell\nu$ a different way to obtain F_L

.. for Marcello

M. Algueró et al. 2003.02533

The angular distribution is (I_i function of $H_{0,+,-,t_i,P}$)

$$\frac{d^4\Gamma}{dq^2 d\cos\theta_D d\cos\theta_\ell d\chi} = \frac{9}{32\pi}\Big\{I_{1c}\cos^2\theta_D + I_{1s}\sin^2\theta_D + \left[I_{2c}\cos^2\theta_D + I_{2s}\sin^2\theta_D\right]\cos 2\theta_\ell$$
$$+\left[I_{6c}\cos^2\theta_D + I_{6s}\sin^2\theta_D\right]\cos\theta_\ell + \left[I_3\cos 2\chi + I_9\sin 2\chi\right]\sin^2\theta_\ell\sin^2\theta_D$$
$$+\left[I_4\cos\chi + I_8\sin\chi\right]\sin 2\theta_\ell\sin 2\theta_D + \left[I_5\cos\chi + I_7\sin\chi\right]\sin\theta_\ell\sin 2\theta_D\Big\},$$

m_ℓ	Tensor ops.	Pseudoscalar op.	Coefficients	Dependencies	Amplitudes	Symmetries
0	No	Yes	11	5	4	2

$$\tilde{F}_L^{D^*} = \frac{d\Gamma_L/dq^2}{\Gamma} = \frac{1}{4\Gamma}(3I_{1c} - I_{2c})$$
$$\tilde{F}_T^{D^*} = \frac{d\Gamma_T/dq^2}{\Gamma} = \frac{1}{2\Gamma}(3I_{1s} - I_{2s})$$

Example: massless, with pseudoscalars no tensors

$$\tilde{F}_T^{D^*} = \frac{1}{\Gamma}2\sqrt{I_3^2 + I_9^2 + \frac{1}{4}I_{6s}^2}$$

Impact of Hadronic Resonances on $B \to K^{(*)}\tau^+\tau^-$ Decays

G. Baltà, A. Crivellin, R. Escribano, J. Matias, M. Novoa-Brunet

based on 2605.21291

Flavorful opportunities in Semileptonic B decays.

The B-Flavour Anomaly Landscape

- Global fits for $b \to s\ell^+\ell^-$ transitions (e.g., P_5', branching ratios) show deviations from the SM exceeding 5σ.

- Tensions in $R(D^{(*)})$ for $b \to c\tau\nu$ transitions persist at $\approx 3\sigma$ to 4σ.

- Tensions in $b \to s\nu\bar{\nu}$ also recently emerged:

$$R^{\nu}_{K^{(*)}} = \frac{\mathcal{B}(B \to K^{(*)}\nu\bar{\nu})}{\mathcal{B}(B \to K^{(*)}\nu\bar{\nu})^{\mathrm{SM}}}$$

SMEFT link

Predicted enhancement consistent with the 90 % *CL* experimental limits:

- $\mathcal{B}(B_s \to \tau^+\tau^-)_{\rm exp} \leq 5 \times 10^{-3}$ (LHCb′17)
- $\mathcal{B}(B \to K\tau^+\tau^-)_{\rm exp} \leq 8.7 \times 10^{-4}$ (Belle I+II′25)
- $\mathcal{B}(B \to K^*\tau^+\tau^-)_{\rm exp} \leq 2.5 \times 10^{-4}$

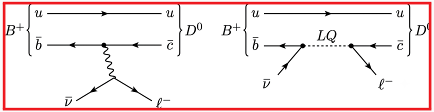

SMEFT Link: Manifest $SU(2)_L$ gauge invariance correlates the left-handed $bc\tau\nu$ current to $b \to s\tau^+\tau^-$ transitions and $b \to s\nu\bar{\nu}$.

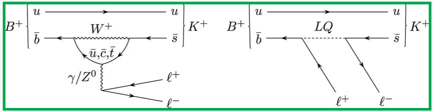

$$\mathcal{O}^{(1)}_{2333} = [\bar{Q}_2\gamma_\mu Q_3][\bar{L}_3\gamma^\mu L_3]$$
$$= [\bar{s}_L\gamma_\mu b_L][\bar{\tau}_L\gamma^\mu \tau_L] + [\bar{s}_L\gamma_\mu b_L][\bar{\nu}_\tau\gamma^\mu \nu_\tau] + \ldots$$

$$\mathcal{O}^{(3)}_{2333} = [\bar{Q}_2\gamma_\mu\sigma^I Q_3][\bar{L}_3\gamma^\mu\sigma^I L_3]$$
$$= 2V_{cs}[\bar{c}_L\gamma_\mu b_L][\bar{\tau}_L\gamma^\mu \nu_\tau] + [\bar{s}_L\gamma_\mu b_L][\bar{\tau}_L\gamma^\mu \tau_L] -$$
$$-[\bar{s}_L\gamma_\mu b_L][\bar{\nu}_\tau\gamma^\mu \nu_\tau] + \ldots$$

NP enhancements of $b \to s\tau^+\tau^-$ up to several orders of magnitude are predicted.

Experimental Challenges in $b \to s\tau^+\tau^-$

- Unlike e and μ modes, τ modes involve missing energy (neutrinos), making q^2 **reconstruction difficult**:
  - While Belle II **can discriminate** q^2 **regions** via tagging,
  - Hadronic environments (LHCb, CMS) **cannot** easily resolve resonances due to the difficult q^2 discrimination.
- **Our Strategy:** Instead of avoiding resonance regions via q^2 cuts, we include resonant contributions (specifically $\psi(2S)$) directly into the predictions for $b \to s\tau^+\tau^-$ with and without NP.

Differential Branching Ratio: Example case $B^+ \to K^+\tau^+\tau^-$

The differential rate is given by:

$$\frac{d\mathcal{B}}{dq^2} = \tau_B \frac{G_F^2 \alpha^2 |V_{tb}V_{ts}^*|^2}{1024\pi^5 m_B^3} \sqrt{\lambda(q^2)}\beta_\tau(q^2) \times$$
$$\left[\frac{2}{3}\lambda(q^2)\beta_\tau^2 |(C_{10}^\tau + C_{10}'^\tau) f_+|^2 + \frac{4m_\tau^2(m_B^2 - m_K^2)^2}{q^2}|(C_{10}^\tau + C_{10}'^\tau) f_0|^2\right.$$
$$\left. + \lambda(q^2)(1 - \frac{1}{3}\beta_\tau^2)\left|(C_{9\tau}^{\text{eff}}(q^2) + C_9')f_+ + \frac{2(C_7^{\text{eff}} + C_7')m_b}{m_B + m_K} f_T\right|^2\right]$$

where $\lambda(q^2)$ is the Källén function and $\beta_\tau(q^2) = \sqrt{1 - 4m_\tau^2/q^2}$.

Require FFs (HPQCD) and WCs.

Treatment of resonances: Data-driven approach

Accurate prediction:

Treatment of resonances: Data-driven approach

Accurate prediction:

1. Compute the local contributions in the standard way.

Treatment of resonances: Data-driven approach

Accurate prediction:

1. Compute the local contributions in the standard way.
2. Include the nonlocal hadronic amplitudes extracted from the fit to $B \to K^{(*)}\mu^+\mu^-$ data from LHCb analysis. **[R. Aaij et al. (LHCb), 2603.12477]** **[R. Aaij et al. (LHCb), JHEP 09, 026]**

   For $B^+ \to K^+\tau^+\tau^-$: $\mathcal{C}_{9\tau}^{\text{eff}}(q^2) = \mathcal{C}_{9\tau} + Y_{c\bar{c}}^{0}(q_0^2) + \Delta Y_{c\bar{c}}^{1\text{p}}(q^2) + \Delta Y_{c\bar{c}}^{2\text{p}}(q^2)$

Treatment of resonances: Data-driven approach

Accurate prediction:

1. Compute the local contributions in the standard way.
2. Include the nonlocal hadronic amplitudes extracted from the fit to $B \to K^{(*)}\mu^+\mu^-$ data from LHCb analysis. **[R. Aaij et al. (LHCb), 2603.12477]** **[R. Aaij et al. (LHCb), JHEP 09, 026]**

   For $B^+ \to K^+\tau^+\tau^-$: $\mathcal{C}_{9\tau}^{\rm eff}(q^2) = \mathcal{C}_{9\tau} + Y_{c\bar{c}}^{0}(q_0^2) + \Delta Y_{c\bar{c}}^{\rm 1p}(q^2) + \Delta Y_{c\bar{c}}^{\rm 2p}(q^2)$

3. Parametrization of the resonances: Dispersion relation method

   $\Delta Y_{c\bar{c}}^{\rm 1p}(q^2) = \sum_j \eta_j e^{i\delta_j} \frac{q^2 - q_0^2}{m_j^2 - q_0^2} A_j^{\rm res}(q^2)\,, \qquad A_j^{\rm res}(q^2) = \frac{m_j \Gamma_{0j}}{m_j^2 - q^2 - i\, m_j \Gamma_j(q^2)}$

   η_j and δ_j are the magnitude and phase of each resonance w.r.t. the local contribution.

Treatment of resonances: Data-driven approach

Accurate prediction:

1. Compute the local contributions in the standard way.
2. Include the nonlocal hadronic amplitudes extracted from the fit to $B \to K^{(*)}\mu^+\mu^-$ data from LHCb analysis. **[R. Aaij et al. (LHCb), 2603.12477]** **[R. Aaij et al. (LHCb), JHEP 09, 026]**

   For $B^+ \to K^+\tau^+\tau^-$: $\mathcal{C}_{9\tau}^{\mathrm{eff}}(q^2) = \mathcal{C}_{9\tau} + Y_{c\bar{c}}^{0}(q_0^2) + \Delta Y_{c\bar{c}}^{1\mathrm{p}}(q^2) + \Delta Y_{c\bar{c}}^{2\mathrm{p}}(q^2)$

3. Parametrization of the resonances: Dispersion relation method

   $\Delta Y_{c\bar{c}}^{1\mathrm{p}}(q^2) = \sum_j \eta_j e^{i\delta_j} \frac{q^2 - q_0^2}{m_j^2 - q_0^2} A_j^{\mathrm{res}}(q^2)\,,\qquad A_j^{\mathrm{res}}(q^2) = \frac{m_j \Gamma_{0j}}{m_j^2 - q^2 - i\, m_j \Gamma_j(q^2)}$

   η_j and δ_j are the magnitude and phase of each resonance w.r.t. the local contribution.

4. Integrate the spectra over the full kinematically allowed range.

Treatment of resonances: Data-driven approach

Accurate prediction:

$$\mathcal{B}(B^+ \to K^+\tau^+\tau^-)_{\rm SM} = 1.86^{+0.17}_{-0.16} \times 10^{-6}$$

$$\mathcal{B}(B \to K^*\tau^+\tau^-)_{\rm SM} = 1.78^{+0.25}_{-0.27} \times 10^{-6}$$

Treatment of resonances: Data-driven approach

Accurate prediction:

$$\mathcal{B}(B^+ \to K^+\tau^+\tau^-)_{\rm SM} = 1.86^{+0.17}_{-0.16} \times 10^{-6}$$

$$\mathcal{B}(B \to K^*\tau^+\tau^-)_{\rm SM} = 1.78^{+0.25}_{-0.27} \times 10^{-6}$$

$q^2_{\rm min}$	$\mathcal{B}(B^+ \to K^+\tau^+\tau^-) \times 10^7$	$\mathcal{B}(B^0 \to K^{*0}\tau^+\tau^-) \times 10^7$
14.18	$1.54\,^{+0.16}_{-0.13}$	$1.54\,^{+0.63}_{-0.45}$
15	$1.37\,^{+0.14}_{-0.12}$	$1.31\,^{+0.55}_{-0.40}$

Including resonances enhances the SM prediction by an order of magnitude compared to short-distance-only calculations.

Spectrum for $B^+ \to K^+\tau^+\tau^-$ and $B \to K^*\tau^+\tau^-$

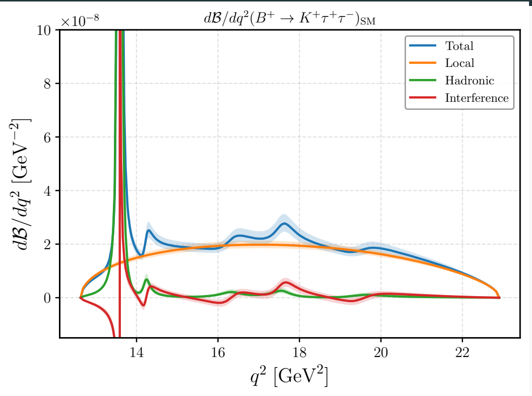

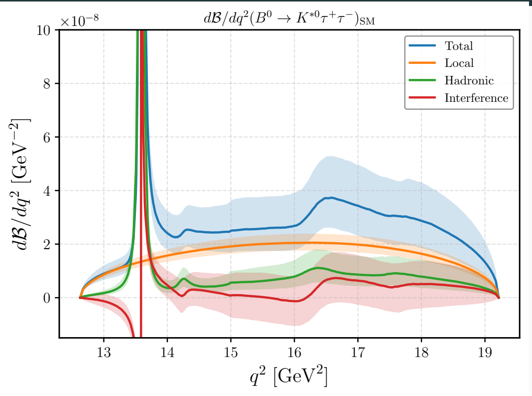

Figure 1: SM Differential Branching Ratio

(Total, Local, Hadronic, and Interference)

- **Interference effects**: While local/hadronic interference is significant near the resonance, it largely cancels when integrated over the full q^2 range due to sign changes across the peak.

Validation via NWA, example of $B^+ \to K^+\tau\tau$

- For narrow resonances like $\psi(2S)$, the Narrow Width Approximation provides a cross-check:

$$\mathcal{B}(B^+ \to K^+\tau^+\tau^-)|_{\text{nl}} \simeq \mathcal{B}(B^+ \to K^+\psi(2S)) \times \mathcal{B}(\psi(2S) \to \tau^+\tau^-)$$

- Conversion from muonic data:

$$\frac{\mathcal{B}(\psi(2S) \to \tau^+\tau^-)}{\mathcal{B}(\psi(2S) \to \mu^+\mu^-)} \simeq \sqrt{1 - \frac{4m_\tau^2}{m_\psi^2}} \left(1 + \frac{2m_\tau^2}{m_\psi^2}\right)$$

- Results from NWA

$$2.09 \pm 0.26 \times 10^{-6}$$

agree well with the full data-driven result

$$1.86 \pm 0.16 \times 10^{-6}$$

Treatment of resonances: Simplified data-independent approach in the NWA

Data-independent (except for the phases) estimate to test the sensitivity of the procedure:

Treatment of resonances: Simplified data-independent approach in the NWA

Data-independent (except for the phases) estimate to test the sensitivity of the procedure:

- Parametrization of the resonances: Dispersion relation (again)

Treatment of resonances: Simplified data-independent approach in the NWA

Data-independent (except for the phases) estimate to test the sensitivity of the procedure:

- Parametrization of the resonances: Dispersion relation (again)
- Extraction of the amplitudes:
  - Magnitudes calculated in the NWA.
  - Phases still taken from the LHCb fit to data.

Treatment of resonances: Simplified data-independent approach in the NWA

Data-independent (except for the phases) estimate to test the sensitivity of the procedure:

- Parametrization of the resonances: Dispersion relation (again)
- Extraction of the amplitudes:
  - Magnitudes calculated in the NWA.
  - Phases still taken from the LHCb fit to data.
- Energy dependence of the running widths ignored.

Treatment of resonances: Simplified data-independent approach in the NWA

Data-independent (except for the phases) estimate to test the sensitivity of the procedure:

- Parametrization of the resonances: Dispersion relation (again)
- Extraction of the amplitudes:
  - Magnitudes calculated in the NWA.
  - Phases still taken from the LHCb fit to data.
- Energy dependence of the running widths ignored.
- 2-particle resonances neglected.

Treatment of resonances: Simplified data-independent approach in the NWA

Data-independent (except for the phases) estimate to test the sensitivity of the procedure:

- Parametrization of the resonances: Dispersion relation (again)
- Extraction of the amplitudes:
  - Magnitudes calculated in the NWA.
  - Phases still taken from the LHCb fit to data.
- Energy dependence of the running widths ignored.
- 2-particle resonances neglected.

$$\mathcal{B}(B^+ \to K^+\tau^+\tau^-) = (2.13 \pm 0.16) \times 10^{-6}$$

Treatment of resonances: Simplified data-independent approach in the NWA

Data-independent (except for the phases) estimate to test the sensitivity of the procedure:

- Parametrization of the resonances: Dispersion relation (again)
- Extraction of the amplitudes:
  - Magnitudes calculated in the NWA.
  - Phases still taken from the LHCb fit to data.
- Energy dependence of the running widths ignored.
- 2-particle resonances neglected.

$$\mathcal{B}(B^+ \to K^+\tau^+\tau^-) = (2.13 \pm 0.16) \times 10^{-6}$$

Accurate prediction

$$\mathcal{B}(B^+ \to K^+\tau^+\tau^-)_{\mathrm{SM}} = 1.86^{+0.17}_{-0.16} \times 10^{-6}$$

Spectra in the Presence of Large NP

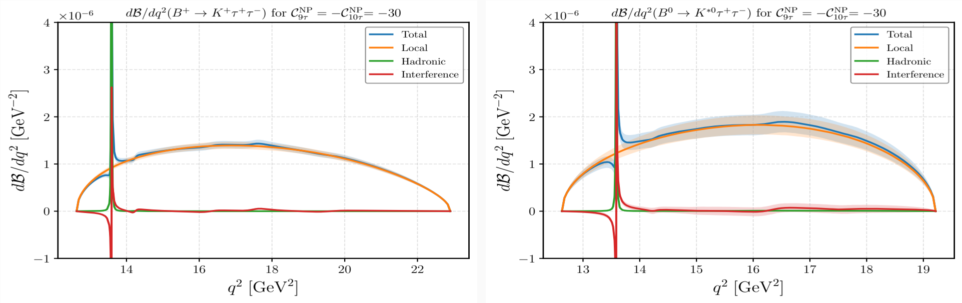

Figure 2: Differential BR for $C_{9\tau}^{\rm NP} = -C_{10\tau}^{\rm NP} = -30$

- **For large NP**, the local (short-distance) integrated contribution becomes comparable to or exceeds the resonant peak.

Quantifying the Resonant Error

We define the relative error δ of neglecting resonances: $\delta \equiv 1 - \frac{\mathcal{B}_{\text{Local}}}{\mathcal{B}_{\text{Total}}}$

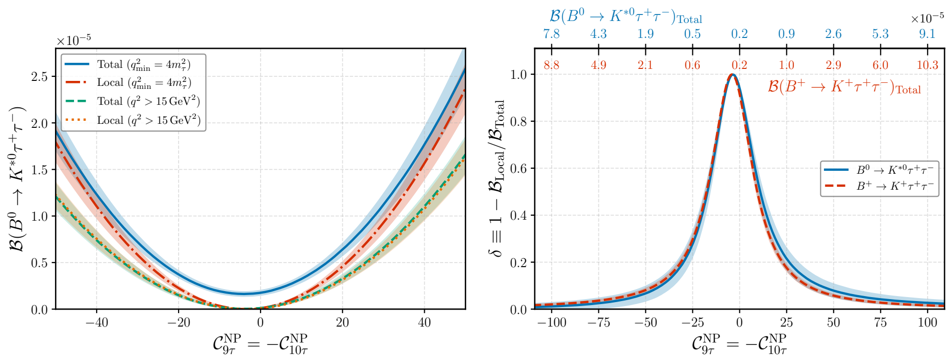

- **Figure 3 (Right):** δ as a function of $C^{\text{NP}}_{9\tau} = -C^{\text{NP}}_{10\tau}$.
- For moderate NP (e.g., $5 \times \text{SM}_{\text{local}}$), the error is still $\approx 20\,\%$.
- Only for very large NP (preferred by some anomalies) does δ drop below $5\,\%$, making the resonance effect negligible.

Branching Ratio as Function of Wilson Coefficients

We provide **explicit dependence** on NP Wilson coefficients $C_{9\tau,10\tau}^{\mathrm{NP}}$:

$$\mathcal{B}(B^+ \to K^+\tau^+\tau^-)_{\mathrm{Total}} = 1.853 \times 10^{-6} + (2.1\, C_{9\tau}^{\mathrm{NP}} - 5.4\, C_{10\tau}^{\mathrm{NP}} + 0.31 (C_{9\tau}^{\mathrm{NP}})^2 + 0.62 (C_{10\tau}^{\mathrm{NP}})^2) \times 10^{-8}$$

$$\mathcal{B}(B^0 \to K^{*0}\tau^+\tau^-)_{\mathrm{Total}} = 1.697 \times 10^{-6} + (4.9\, C_{9\tau}^{\mathrm{NP}} - 1.7\, C_{10\tau}^{\mathrm{NP}} + 0.63 (C_{9\tau}^{\mathrm{NP}})^2 + 0.20 (C_{10\tau}^{\mathrm{NP}})^2) \times 10^{-8}$$

Notice that for $C_{9\tau}^{\mathrm{NP}} = -C_{10\tau}^{\mathrm{NP}} < 0$ one finds for K^+ that the BR only raises starting at $|C_{9\tau}^{\mathrm{NP}}| \geq 9$ and for K^* starting at $|C_{9\tau}^{\mathrm{NP}}| \geq 6$.

These are essential for directly comparing experimental results to SMEFT scenarios.

Correlations with $R(D^{(*)})$ and $B \to K^{(*)}\nu\nu$

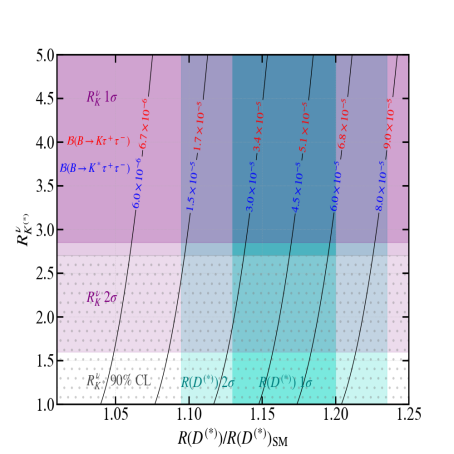

- Left-handed vector operators $O^{(1)}_{2333}$ and $O^{(3)}_{2333}$ link $b \to c\tau\nu$ and $b \to s\nu\nu$ with $b \to s\tau^+\tau^-$.
- **Figure:** Predictions for $\mathcal{B}(B \to K^{(*)}\tau^+\tau^-)$ as a function of $R(D^{(*)})/R(D^{(*)})_{\rm SM}$ and $R^\nu_{K^{(*)}}$.
- For currently preferred values of $R(D^{(*)})$ and R^ν_K, the predicted branching ratio is a few times 10^{-5}.

Conclusions and Outlook

- Integrating over the **full phase space** from $4\ m_\tau^2$ is necessary for comparisons with LHCb and CMS.
- The $\psi(2S)$ resonance enhances SM branching ratios by an order of magnitude.
- Neglecting the resonance can lead to errors of $\approx 20\,\%$ even for moderate NP contributions ($C_{9\tau}^{\mathrm{NP}} \simeq -25$).
- This data-driven approach is also applicable to $B_s \to \phi\tau^+\tau^-$ and $\Lambda_b \to \Lambda\tau^+\tau^-$.
- These predictions provide the necessary SM baseline for upcoming experimental measurements in the tauonic sector.

Probing Unknown Nonperturbative Effects in $b \to s\ell\ell$

Inclusive vs. Exclusive Observables and the C_9 Dilemma

P. Alvarez-Cartelle, B. Capdevila, E. Lunghi, and J. Matias

based on arxiv 2605.06567

Flavorful opportunities in Semileptonic B decays.

Motivation: The C_9 Dilemma

- **Experimental Status:** Persistent discrepancies in $b \to s\mu\mu$ transitions: P_5' angular observable, deficits in branching ratios of $B \to K\mu\mu$, $B \to K^*\mu\mu$, and $B_s \to \phi\mu\mu$.
- **Global Fits:** Consistently prefer a universal shift in C_9 ($C_9^{\mathrm{NP}} \approx -1.16$).
- **The Core Question:** Is this New Physics or a hypothetical constant, universal hadronic contribution ("charming penguins") mimicking New Physics?.
- **Objective:** Use the distinct theoretical sensitivity of inclusive vs. exclusive modes to disentangle these possibilities.

Theoretical Framework: Effective Hamiltonian

The weak effective Hamiltonian for $b \to s\ell\ell$ is defined as:

$$\mathcal{H}_{\text{eff}} = -\frac{4G_F}{\sqrt{2}} V_{tb} V_{ts}^* \sum_i C_i \mathcal{O}_i + \text{h.c.} \tag{1}$$

The semileptonic operator of interest is:

$$\mathcal{O}_{9\ell} = \frac{e^2}{16\pi^2} (\bar{s}\gamma_\mu P_L b)(\bar{\ell}\gamma^\mu \ell) \tag{2}$$

Non-local QCD effects (charm loops) generate an effective shift:

$$C_9^{\text{eff}} = C_9^{\text{pert}} + C_9^{\text{non-local}}$$

where C_9^{pert} contains among others C_9^{SM} (local) and C_9^{NP}.

Theory Control: Inclusive vs. Exclusive

Exclusive ($B \to K^{(*)}\ell\ell$)

- **Low q^2:** SCET-II framework; power corrections involve non-local form factors ("charming penguins"). Inputs: Form Factors, LCDA.
- **High q^2:** $1/q^2$ expansion (OPE in q^2): only integrated spectrum; local power corrections only. Inputs: Form Factors, HQET matrix elements.

-Form Factors:

- LCSR (B-meson DA or light-meson DA)
- Lattice QCD.

Inclusive ($B \to X_s\ell\ell$)

- **Global OPE:** Described by HQE.
- **Krüger-Sehgal (KS) Mechanism:** Factorizable charm loops determined exactly from $e^+e^- \to$ hadrons data used to incorporate resonances.

- **Low-q^2**: OPE, Leading uncertainties: **Resolved Photons:** Subleading power corrections at low q^2 estimated at $\sim 5\,\%$.
- **High-q^2**: OPE breaks down but the ratio $b \to s\ell\ell/b \to u\ell\nu$ is well behaved with some cuts. Leading uncertainties: $\mathcal{O}(1/m_b^3)$ HQET ME (WA).

Inclusive

OPE free of uncertainties up to power corrections

$$\Gamma[B \to X_s \ell\ell] = \Gamma[b \to X_s \ell\ell] + \mathcal{O}(\frac{\Lambda^2_{QCD}}{m_b^2}, \frac{\Lambda^2_{QCD}}{m_c^2})$$

However due to the expansion parameter (from p^2_{Xs})

$$\frac{\Lambda_{QCD}}{m_b - \sqrt{q^2}}$$

OPE breaks down at high-q^2 generating power corrections.

...Cured normalising to $\bar{B}^0 \to X_u \ell \nu$ with identical power corrections (WA ME cancel)

Inclusive resonances

They are incorporated using $e^+e^- \to$ hadrons data (BESII, Babar, ALEPH...)

...using Krüger-Sehgal mechanism that works nicely for inclusive.

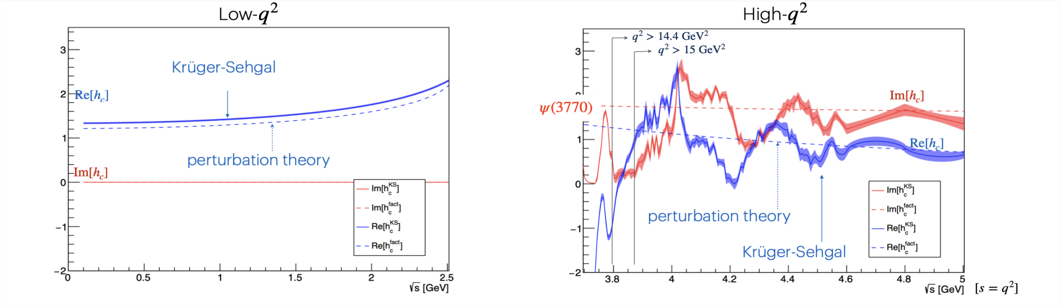

Finally, non-resonant color-octet effects:

- at high-q^2 can be calculated in PT and scale as Λ^2_{QCD}/q^2 **[Buchalla, Isidori, Rey]** and
- at low-q^2 can be treated with SCET **[Hurth, Turczyk et al]**, required a cut on m_X and lead to resolved contributions (5 %).

Exclusive issues: non-local power corrections

Non-local matrix elements $< B|TJ_\mu^{em} O_2|B >$:

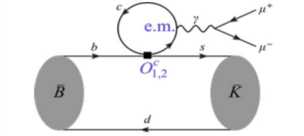

Contains: - Simple diagram included in factorization formula, - Hard gluon exchange also included in QCDF and - soft gluon emitted by the $c\bar{c}$ loop estimated by **Khodjamirian et al.** and at NLO by **Van Dyk et al.** (substantial cancellation). **All of them are included in SM predictions.**

It was hypothesized that triangle diagrams could explain data due to possible large anomalous thresholds:

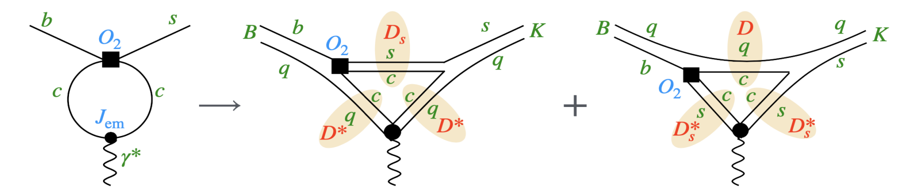

Two important points why those triangle diagrams are probably not the answer

Point 1: Clash with Global fits that show **same deficit** at large and low q^2 while DD_s^* and D_sD^* rescattering computed by **[Bordone, Isidori, Machler, Tinari]** show opposite sign (monopole dominant) and same(dipole) and global fits require $|\delta C_9/C_9| \simeq 0.25$:

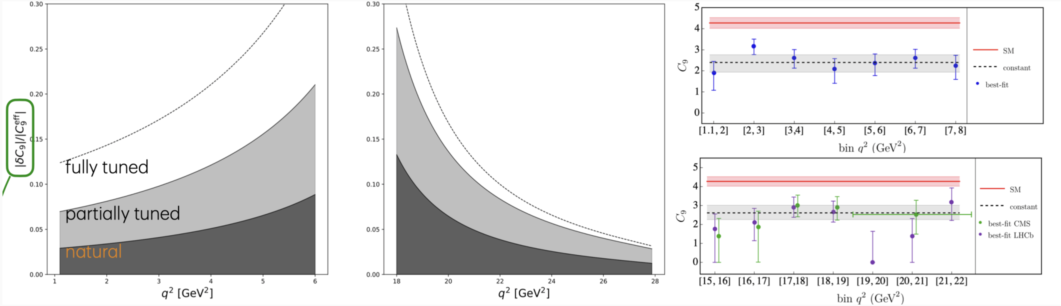

Point 2: The structure of anomalous thresholds of the hadronic and partonic diagram are **exactly the same** **[Mutke et al. 2406.14608, Hoferichter et al. 2604.01284]**. Double counting?

Still....

Can one distinguish an unknown hadronic contribution (different from the previous) coming from (?) that is universal in q^2 and mode-independent?

$$\mathcal{C}_{9\ell}^{\rm eff} \to \mathcal{C}_{9\ell}^{\rm eff} = \mathcal{C}_{9\ell,\,\rm pert}^{\rm SM} + \mathcal{C}_{9\ell}^{\rm NP} + \mathcal{C}_{9,j}^{c\bar{c}\,B\to K^{(*)}}$$

where $j = \perp, \|, 0$ **and**

$$\mathcal{C}_{9\ell,\,\rm pert}^{\rm SM} = \mathcal{C}_{9\ell}^{\rm SM} + Y(q^2)$$

Adding an extra piece that would compete with $\mathcal{C}_{9\ell}^{\rm NP}$:

$$\mathcal{C}_{9,\rm extra}^{K^{(*)},\rm high} = \mathcal{C}_{9,\rm extra}^{K^{(*)},\rm low} = \mathcal{C}_{9,\rm extra}$$

Still....

Can one distinguish an unknown hadronic contribution (different from the previous) coming from (?) that is universal in q^2 and mode-independent?

$$\mathcal{C}_{9\ell}^{\text{eff}} \to \mathcal{C}_{9\ell}^{\text{eff}} = \mathcal{C}_{9\ell,\,\text{pert}}^{\text{SM}} + \mathcal{C}_{9\ell}^{\text{NP}} + \mathcal{C}_{9,j}^{c\bar{c}\,B\to K^{(*)}}$$

where $j = \perp, \|, 0$ **and**

$$\mathcal{C}_{9\ell,\,\text{pert}}^{\text{SM}} = C_{9\ell}^{\text{SM}} + Y(q^2)$$

Adding an extra piece that would compete with $\mathcal{C}_{9\ell}^{\text{NP}}$:

$$\mathcal{C}_{9,\text{extra}}^{K^{(*)},\text{high}} = \mathcal{C}_{9,\text{extra}}^{K^{(*)},\text{low}} = \mathcal{C}_{9,\text{extra}}$$

YES

Proposed Observables: The $\mathcal{F}$ Ratios to test unknown rescattering effects

Ratios of exclusive to inclusive branching fractions designed to cancel normalization uncertainties and be sensitive to $\mathcal{C}_{9,\mathrm{extra}}$ dependence:

Definitions

$$\mathcal{F}_{K^{(*)}}^{[1.1,6]} = \frac{\mathcal{B}(B \to K^{(*)}\mu\mu)_{[1.1,6]}}{\mathcal{B}(B \to X_s \ell\ell)_{[1,6]}} \quad \text{and} \quad \mathcal{F}_{K^{(*)}}^{>15} = \frac{\mathcal{B}(B \to K^{(*)}\mu\mu)_{>15}}{\mathcal{B}(B \to X_s \ell\ell)_{>15}}$$

The Logic: Exclusive modes are sensitive to hypothetical hadronic shifts $C_{9,\mathrm{extra}}$; inclusive modes are not. These ratios have **reduced sensitivity to universal NP** due to partial numerator-denominator cancellation.

No need of external normalizations, it can be measured in house

Experimental Results for $\mathcal{F}$ Ratios

Comparison of current experimental determinations vs. theoretical scenarios:

	$\mathcal{F}_K^{>15}$	$\mathcal{F}_{K^*}^{>15}$	$\mathcal{F}_K^{[1.1,6]}$	$\mathcal{F}_{K^*}^{[1.1,6]}$
$(\mathcal{C}_9^{\mathrm{NP}}, \mathcal{C}_{9,\mathrm{extra}}) = (0,0)$	0.270(64)	0.64(14)	0.099(11)	0.109(60)
$(\mathcal{C}_9^{\mathrm{NP}}, \mathcal{C}_{9,\mathrm{extra}}) = (-1.16,0)$	0.271(64)	0.65(14)	0.0928(98)	0.112(62)
$(\mathcal{C}_9^{\mathrm{NP}}, \mathcal{C}_{9,\mathrm{extra}}) = (0,-1.16)$	0.210(50)	0.50(11)	0.0764(81)	0.092(51)
experiment	**0.309(15)**	**0.629(21)**	**0.084(13)**	**0.110(17)**

Theoretical determinations of the ratios $\mathcal{F}_{K^{(*)}}^{[1.1,6],>15}$ for various values of $\mathcal{C}_9^{\mathrm{NP}}$ and $\mathcal{C}_{9,\mathrm{extra}}$ and comparison to their current experimental determinations. Notice that, by construction, the sensitivity to NP is almost flat.

Insight: High q^2 ratios show a slight preference for NP (1.9σ against hadronic for $F_K^{>15}$).

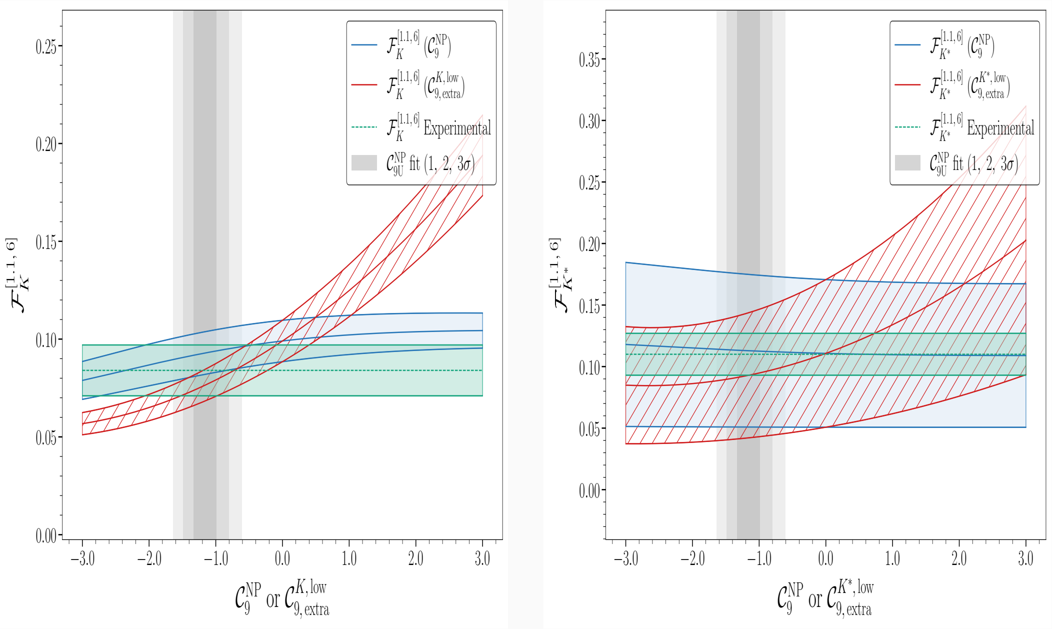

$\mathcal{F}_K^{[1.1,6]}\,(\mathcal{C}_9^{\mathrm{NP}})$
$\mathcal{F}_K^{[1.1,6]}\,(\mathcal{C}_{9,\mathrm{extra}}^{K,\mathrm{low}})$
$\mathcal{F}_K^{[1.1,6]}$ Experimental
$\mathcal{C}_{9U}^{\mathrm{NP}}$ fit (1, 2, 3σ)
$\mathcal{F}_K^{[1.1,6]}$
$\mathcal{C}_9^{\mathrm{NP}}$ or $\mathcal{C}_{9,\mathrm{extra}}^{K,\mathrm{low}}$
$\mathcal{F}_{K^*}^{[1.1,6]}\,(\mathcal{C}_9^{\mathrm{NP}})$
$\mathcal{F}_{K^*}^{[1.1,6]}\,(\mathcal{C}_{9,\mathrm{extra}}^{K^*,\mathrm{low}})$
$\mathcal{F}_{K^*}^{[1.1,6]}$ Experimental
$\mathcal{C}_{9U}^{\mathrm{NP}}$ fit (1, 2, 3σ)
$\mathcal{F}_{K^*}^{[1.1,6]}$
$\mathcal{C}_9^{\mathrm{NP}}$ or $\mathcal{C}_{9,\mathrm{extra}}^{K^*,\mathrm{low}}$

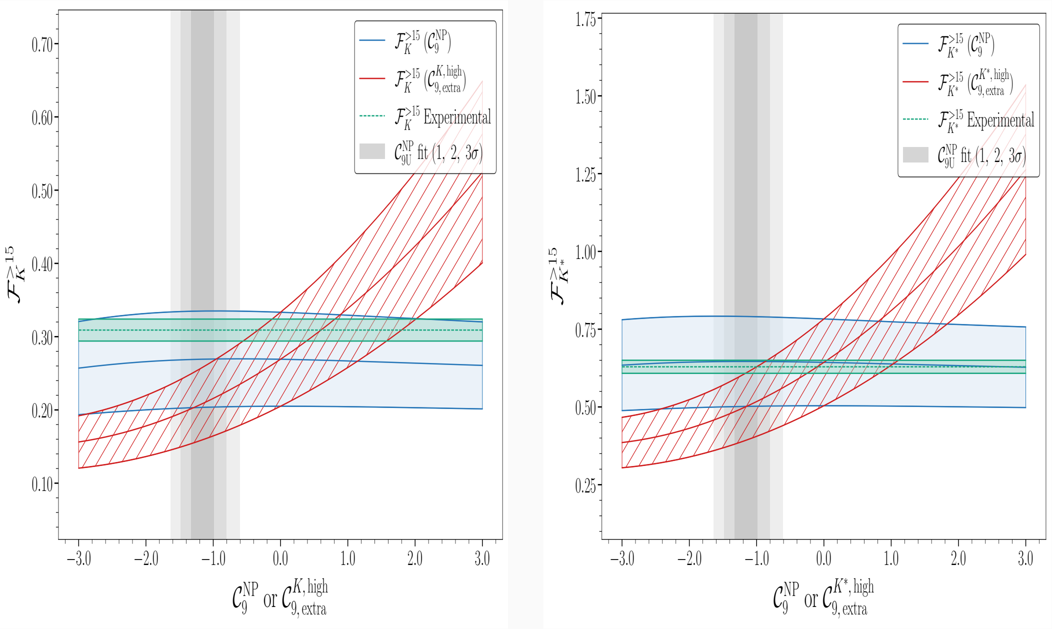

$\mathcal{F}_K^{>15}\ (\mathcal{C}_9^{\rm NP})$
$\mathcal{F}_K^{>15}\ (\mathcal{C}_{9,\rm extra}^{K,\rm high})$
$\mathcal{F}_K^{>15}$ Experimental
$\mathcal{C}_{9\rm U}^{\rm NP}$ fit (1, 2, 3σ)
$\mathcal{F}_K^{>15}$
$\mathcal{C}_9^{\rm NP}$ or $\mathcal{C}_{9,\rm extra}^{K,\rm high}$
$\mathcal{F}_{K^*}^{>15}\ (\mathcal{C}_9^{\rm NP})$
$\mathcal{F}_{K^*}^{>15}\ (\mathcal{C}_{9,\rm extra}^{K^*,\rm high})$
$\mathcal{F}_{K^*}^{>15}$ Experimental
$\mathcal{C}_{9\rm U}^{\rm NP}$ fit (1, 2, 3σ)
$\mathcal{F}_{K^*}^{>15}$
$\mathcal{C}_9^{\rm NP}$ or $\mathcal{C}_{9,\rm extra}^{K^*,\rm high}$

Consistency Test at high-q^2: Sum of Exclusive vs. OPE (Inclusive)

At high q^2, the inclusive rate is essentially saturated by summing K, K^*, $(K\pi)_S, K\pi\pi$ ($< 3\,\%$):

- **Theoretical Consistency:** How the OPE inclusive prediction with Σ of exclusive modes compare?. This requires to add also the dependence of this residual branching ratio on $\mathcal{C}_9^{\mathrm{NP}}$ and $\mathcal{C}_{9,\mathrm{extra}}$ **G.Isidori et al. 2305.03076 (central value)**

$$10^7 \times \mathcal{B}_{\mathrm{rest}>15} = 0.547 + 0.124\,(\mathcal{C}_9^{\mathrm{NP}} + \mathcal{C}_{9,\mathrm{extra}}) + 0.015\,(\mathcal{C}_9^{\mathrm{NP}} + \mathcal{C}_{9,\mathrm{extra}})^2\,.$$

This amounts to $13\,\%$ of the total sum of exclusive channels and is more uncertain.

	Region (q^2)	α	β	γ
$10^7 \times \mathcal{B}\,(B \to K\mu\mu)$	> 15	1.105	0.252	0.033
$10^7 \times \mathcal{B}\,(B \to K^*\mu\mu)$	> 15	2.640	0.600	0.082
$10^7 \times \mathcal{B}\,(B \to K\pi\mu\mu)$	> 15	0.547	0.124	0.015
$10^7 \times \mathcal{B}\,(B \to X_s\mu\mu)$ (sum excl)	> 15	4.292	0.976	0.130
$10^7 \times \mathcal{B}\,(B \to X_s\mu\mu)$ (incl)	> 15	4.10	0.96	0.14

$$10^7\mathcal{B}_{\sum \mathrm{exc}} \simeq 4.29 + 0.98\,C_9^{\mathrm{NP}} + 0.13(C_9^{\mathrm{NP}})^2 \quad \text{vs.} \quad 10^7\mathcal{B}_{\mathrm{incl}} \simeq 4.10 + 0.96\,C_9^{\mathrm{NP}} + 0.14(C_9^{\mathrm{NP}})^2$$

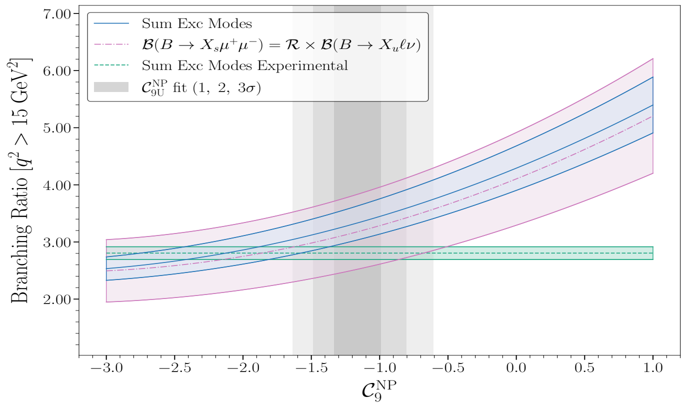

Figura 4: $B \to X_s\mu\mu$ branching ratio for $q^2 > 15\ \mathrm{GeV}^2$ calculated using the OPE ($\mathcal{R} \times \mathcal{B}_{u\ell\nu}$) or as a sum of exclusive and comparison with the experimental determination.

The inclusive isospin-averaged **high-q^2** branching ratio as sum of exclusive can be written as:

$$10^7\mathcal{B}(B \to X_s\mu\mu)_{\rm exp} = \tilde{\mathcal{B}}(B \to K\mu\mu) + \tilde{\mathcal{B}}(B \to K^*\mu\mu) + \tilde{\mathcal{B}}(B \to (K\pi)_S\mu\mu) + \tilde{\mathcal{B}}(B \to K\pi\pi\mu\mu)$$

$$= (2.80 \pm 0.11) \quad \text{vs} \quad \tilde{\mathcal{B}}[>15]^{\rm inc}_{\rm SM} = (4.10 \pm \mathbf{0.81})(1.6\sigma) \text{ and } \tilde{\mathcal{B}}[>15]^{\rm exc}_{\rm SM} = (4.29 \pm \mathbf{0.39})(3.7\sigma)$$

Disfavoring the Hadronic Scenario: A different type of comparison

Using the branching ratios of exclusive and inclusive we can impose two conditions on the constant universal $C_{9,\text{extra}}$:

- **First condition**:
$$(\mathcal{B}_{\text{SM}}^{\sum \text{exc}} - \mathcal{B}^{\sum \text{exc,exp}}) = 0,$$
$C_{9,\mathrm{extra}}$ has to be in agreement with data. If we assume no NP $\Rightarrow$ $C_{9,\mathrm{extra}} = -1.16$
- **Second condition**: $C_{9,\text{extra}}$ has to be adjusted to fulfill:
$$(\mathcal{B}_{\text{SM}}^{\sum \text{exc}} - \mathcal{B}_{\text{SM}}^{\text{inc}}) = 0.$$
If we impose that both computations must agree one finds at 68 % CL
$$\mathcal{C}_{9,\mathrm{extra}} = -0.20^{+0.90}_{-1.10}.$$
If we assume a reduction of 50 % in this error thanks to improvement on $\mathcal{B}(B \to X_u \ell \nu)$ measurement and the central value remains untouched one finds at 68 % CL
$$\mathcal{C}_{9,\mathrm{extra}} = -0.20^{+0.59}_{-0.62}.$$

compatible with zero and in tension with the value required to explain anomalies.

A comparison at the level of C_9-dependencies

We now turn to **a different comparison:** normalization-independent ratios $R_X = \mathcal{B}_X/\mathcal{B}_{X,\mathrm{SM}}$ to compare $\mathcal{C}_9$ dependencies of the inclusive mode and the sum of exclusive modes.

$$\begin{aligned} R^{\rm inc} &= \frac{\mathcal{B}^{\rm inc}}{\mathcal{B}^{\rm inc}_{\rm SM}} = 1 + 0.234\,\mathcal{C}_9^{\rm NP} + 0.034\,{\mathcal{C}_9^{\rm NP}}^2, \\ R^{\sum exc} &= \frac{\mathcal{B}^{\sum \rm exc}}{\mathcal{B}^{\sum \rm exc}_{\rm SM}} = \frac{1 + 0.227(\mathcal{C}_9^{\rm NP} + \mathcal{C}_{9,\rm extra}) + 0.030(\mathcal{C}_9^{\rm NP} + \mathcal{C}_{9,\rm extra})^2}{1 + 0.227\mathcal{C}_{9,\rm extra} + 0.030\mathcal{C}_{9,\rm extra}^2}. \end{aligned}$$

The two limiting scenarios of interest are: i) $\mathcal{C}_9^{\rm NP} = 0$, then $C_{9,\rm extra}$ mimics NP, implying $R^{\sum exc} = 1$, and ii) $\mathcal{C}_{9,\rm extra} = 0$, the purely NP case.

The corresponding experimental value is

$$R^{\rm exp} = \frac{\mathcal{B}^{\sum \rm exc,exp}}{\mathcal{B}^{\rm inc}_{\rm SM}} = 0.68 \pm 0.14,$$

- **The Conflict:** Switching on $C_{9,\text{extra}}$ increases the tension between the inclusive OPE calculation and the sum of measured exclusive channels.
- **Data** The purely hadronic contribution, i.e, $R^{\sum \text{exc}} = 1$ is in tension with the experimental band at 2.3σ

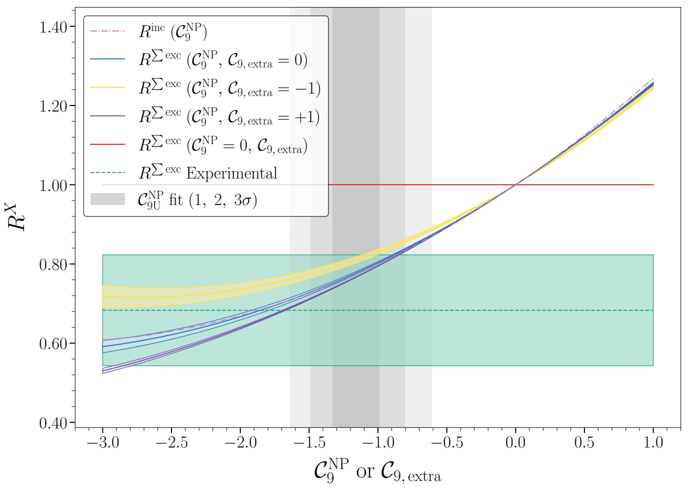

Future Projections: Belle II & LHCb

Inclusive Measurement: Dominant uncertainty from the inclusive BUT:

- at **low-q^2** Inclusive (stat. limited) at present (400 fb^{-1}) end of year ($1\ ab^{-1}$) uncertainties of $\mathcal{F}_{K^{(*)}}^{[1.1,6]}$ about 10 % pretty soon.

Belle II improved measurement of $\mathcal{B}(B \to X_u \ell \nu)$ will strongly impact on inclusive uncertainty.

Parametric Inputs: Improved determinations of $|V_{ub}|$ and vacuum annihilation matrix elements from Lattice QCD.

Outcome: Uncertainties at **high-q^2** $\mathcal{F}$ ratios expected to improve by $> 50\,\%$ in the near future.

LHCb Reach: High q^2 $\mathcal{F}$ ratios can be measured directly by LHCb without external charmonium normalizations.

Conclusions

- **Methodology:** The F observables provide a robust test to distinguish NP from constant universal hadronic effects.
- **Findings:** Current data disfavors a purely hadronic solution to the B-anomalies. Universal $C_{9,\text{extra}}$ breaks the consistency between OPE-based inclusive rates and measured exclusive sums.
- **Outlook:** The imprint of New Physics is distinguishable from hadronic shifts when inclusive modes are included.

BACK-UP SLIDES

Observable bounds

We can calculate the bounds of the observables from the observables derived from the moments:

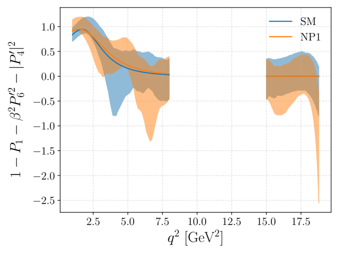

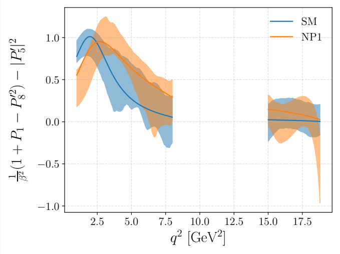

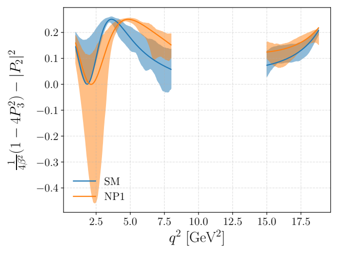

- Note these are single toys
  - The moments are independently obtained with no prior knowledge of the bounds
  - The bounds may be violated locally due to statistical uncertainty
  - For an analysis one evaluates how much a bound may be violated for a given data set

Adding

We don't have to limit ourselves to !

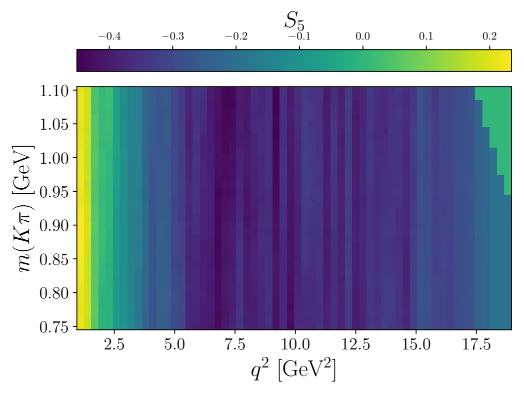

Pseudo-experiment generated with BW in , factorising with Ω and .

- We can study the observables, completely model-independently, as a function of
- We can even study and together
- Are the angular observables really constant across ?
  - If not, does that have implications for their interpretation?

Final points and outlook

- This can be done with other modes
  - $\rightarrow$ is a candidate with only one partial wave to contend with
  - Similarly $\rightarrow$ with a small sample size
  - Potentially a route in for $\rightarrow$ angular analyses - to be studied
- The acid test is the precision on the WCs
  - Work ongoing to incorporate the results of such an unbinned moments analysis into a WC fit
  - Sample the curves at a large number of points and assess the correlations between them

Normalization and Isospin Breaking

- Experimental branching ratios often assume $f_{+-} = f_{00} = 1/2$ for $\Upsilon(4S) \to B\bar{B}$ [21].
- This work performs a profile log-likelihood fit to correct these fractions [21, 22]:

$$f_{+-} = 0.511 \pm 0.010, \quad f_{00} = 0.4851 \pm 0.0088 \tag{3}$$

- **Updated Averages:** Normalization modes like $B \to J/\psi K^{(*)}$ are rescaled, significantly impacting absolute branching ratio determinations [23-25].

(Refer to Figure 2: Profile Likelihood of f_{+-} and f_{00}) [26].

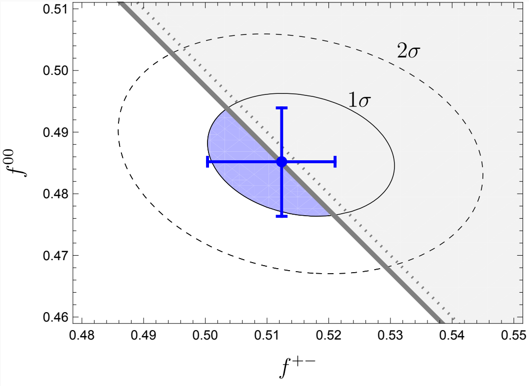

Figura 6: Result of the profile log-likelihood fit following the strategy presented in Ref. [**?**]. The two contours correspond to $\chi^2_{\rm min} + 1$ and $\chi^2_{\rm min} + 4$. The gray region is excluded by a lower limit on $f_{\not B}$ and causes the asymmetry in the fit result (in blue).

Treatment of Non-local Hadronic Effects

- We use a **data-driven approach** based on LHCb fits to $B \to K^{(*)}\mu^+\mu^-$.
- The non-local amplitudes (including phases) are lepton-flavour universal (up to QED) and are transferred to the tauonic mode.
- **Effective Wilson Coefficient** $C_{9\tau}^{\text{eff}}(q^2)$:

$$C_{9\tau}^{\text{eff}}(q^2) = C_{9\tau} + Y_{c\bar{c}}^{0}(q_0^2) + \Delta Y_{c\bar{c}}^{1p}(q^2) + \Delta Y_{c\bar{c}}^{2p}(q^2)$$

- The one-particle contribution uses a relativistic Breit-Wigner (BW) model:

$$\Delta Y_{c\bar{c}}^{1p}(q^2) = \sum_j \eta_j e^{i\delta_j} \frac{q^2 - q_0^2}{m_j^2 - q_0^2} \frac{m_j \Gamma_{0j}}{m_j^2 - q^2 - i m_j \Gamma_j(q^2)}$$